Experimental and theoretical study of the morphology of commensurate and incommensurate graphene layers on Ni single-crystal surfaces

D. Usachov,[1,*] A. M. Dobrotvorskii,[1] A. Varykhalov,[1,2] O. Rader,[2] W. Gudat,[2] A. M. Shikin,[1] and V. K. Adamchuk[1]
[1]*Institute of Physics, St. Petersburg State University, St. Petersburg 198504, Russia*
[2]*BESSY, D-12489 Berlin, Germany*
(Received 24 March 2008; published 1 August 2008)

The paper reports on a scanning tunneling microscopy (STM) study and computer simulation with an N-body interatomic interaction potential of a graphite monolayer (i.e., graphene) on the Ni(111), (110), (755), and (771) single-crystal surfaces. Unlike the case of graphene on Ni(111), which forms a solid single-crystal coating with (1×1) structure, graphene on the Ni(110) surface forms a complex crystal structure distorted substantially by interaction with the substrate. Calculations of the graphene/Ni(110) system have revealed that the strong chemical interaction of carbon with nickel gives rise to a noticeable curving of the graphene layer on a scale of a few angstroms. The model thus derived has permitted proper interpretation of the experimental data obtained by STM, as well as prediction of the main result of studies of graphene formed on faceted surfaces, which have revealed the ability of graphene to coat geometrically nonuniform surfaces in the form of a curved continuous film.

DOI: 10.1103/PhysRevB.78.085403 PACS number(s): 68.43.Fg, 68.55.J−, 68.37.Ef

I. INTRODUCTION

A lot of low-dimensional carbon systems with atomic structures similar to that of graphite are presently known. The quasi-two-dimensional nature of the graphite lattice makes the existence of graphene, i.e., graphite monolayer, as an individual structure possible. The interest toward the investigation of graphene is stimulated, on the one hand, by its low dimension and a number of unique properties of different carbon systems revealed recently, such as superconductivity[1–3] and an anomalous quantum Hall effect.[4–7] On the other hand, studies of graphene may give a key to understanding the properties of other carbon nanostructures, such as the fullerenes and carbon nanotubes, which resemble in some respects curved fragments of graphene. Graphene has been isolated only recently,[8] and its properties have been recovered when grown on SiC surfaces.[9,10] We have been preparing graphene on the surface of metals. Graphite-metal systems promise a considerable application potential in the area of heterogeneous catalysis. Indeed, the stability and service lifetime of metal catalysts employed in processing raw hydrocarbons is determined in a large measure by their stability against blocking of their surface by adsorbed products of dehydropolycyclization of hydrocarbons, which have graphitelike structure.[11] A problem plaguing hydrogen energetics is proper deactivation of nickel catalysts employed in methane steam reforming process, a key stage in hydrogen production.[12]

Theoretical studies of the mechanisms underlying the operation of nickel catalysts in steam reforming suggest that it is surface defects, in particular, atomic steps that are the most active catalytic sites.[13] They are also of a great importance in the process of nickel graphitization because they initiate growth of the grapheme.[13,14] At the same time, in most of the experimental studies of graphene it was synthesized on flat surfaces only. In the particular case of a nickel substrate, graphene was studied in considerable detail on the (111) plane where it forms a commensurate overlayer with (1×1) structure.[15,16] Valuable information was obtained on the crystal and electronic structure and phonon spectra of graphene on Ni(111),[15–20] as well as on their variation under intercalation with atoms of different types.[21–29] Reports on the structure of graphene on more complex crystal faces are few in number.[30] This accounts for the interest aroused by studies of the structure of graphene on other flat incommensurate faces, as well as on geometrically nonuniform metal surfaces approaching the real structure of catalysts.

The present paper reports on an experimental study by scanning tunneling microscopy (STM) and mathematical simulation of the structure of graphene layers grown on surfaces with a complex geometry, including those with lattice parameters different from that of graphite. Crystal planes with high Miller indices (stepped surfaces) were used to model a geometrically nonuniform surface. Our earlier study revealed that such nickel surfaces coated by graphene are faceted, i.e., they have a complex relief formed by different low-index faces.[31] A total of four types of substrates have been investigated: (i) a planar Ni(111) surface with crystal structure close to that of graphite, i.e., having the same hexagonal cell symmetry and similar lattice constants, (ii) a planar Ni(110) surface with the symmetry of a rectangular network, (iii) a stepped Ni(755) surface with (111) basal terrace, which undergoes faceting during graphene synthesis to convert essentially to alternating (111) and (311) faces, and (iv) a stepped Ni(771) surface, which is similar in structure to Ni(755) and is also faceted, the step terraces of which are formed by the (110) and (331) planes. To determine the structure of graphene on the nickel surface on an atomic level, a computer simulation of the equilibrium atomic configuration of the graphene layer on the Ni(110) surface has been performed.

II. EXPERIMENTAL CONDITIONS

Atomically clean, well ordered Ni(755), Ni(771), and Ni(110) surfaces were prepared in ultrahigh vacuum by al-

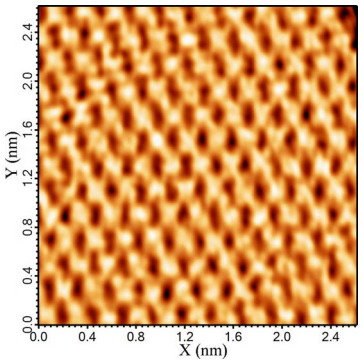

FIG. 1. (Color online) STM image of graphene on Ni(111) (current channel, $V=20$ mV, $I=20$ nA).

ternately subjecting single-crystal surfaces to Ar+ ion sputtering and short heating up to a temperature of about 600 °C. To remove carbon atoms from the surface, the sample was annealed in an oxygen environment at a partial pressure of 5×10^{-8} mbar and sample temperature of 450 °C for 10 min. The stepped Ni(755) and Ni(771) surfaces were obtained by cutting the surfaces of Ni single crystals at angles of 9.45° for Ni(755) and 5.77° for Ni(771) with respect to the Ni(111) and Ni(110) basal planes, accordingly. The geometric structure of such surfaces is formed by periodic steps of monatomic height. The terraces between the steps have the structure of the basal Ni(111) and Ni(110) surfaces. The step periodicity, determined by the basal plane and the cut angle, is 12.4 Å for both Ni(755) and Ni(771) surfaces. The structure and quality of the surfaces thus prepared was checked by low-energy electron diffraction (LEED). Graphene was formed on the nickel surfaces by propylene cracking at a partial propylene pressure of 10^{-6} mbar, sample temperature of 480 °C, and exposure time of 5 min. This self-limited reaction results in formation of a single graphite layer. The surface geometry was studied by scanning tunneling microscopy (Omicron VT SPM) at a base pressure of not more than 2×10^{-10} mbar.

III. EXPERIMENTAL RESULTS

A. Structure of graphene on flat Ni(111) and Ni(110) surfaces

The structure of graphene grown on a flat Ni(111) surface is well known.[16] Since the lattices of the adsorbate and of the substrate have similar lattice parameters, graphene forms the (1×1) structure. The coating is continuous and has nearly single-crystal structure. Figure 1 displays an STM image of graphene on the Ni(111) surface. With the measurement parameters used, the pattern of the STM image does not reproduce correctly the atomic structure of the surface. The image shows a hexagonal structure corresponding to the graphite lattice (similar to the case of pure graphite).

The structure of graphene formed on the planar Ni(110) surface is radically different. A typical LEED pattern obtained for this system (Fig. 2) evidences a domain structure of the graphene. Graphene can exist in three preferred orientations with respect to the substrate [with the corresponding reflections labeled in Fig. 2(b) by 1, 2, and 3]. An analysis of

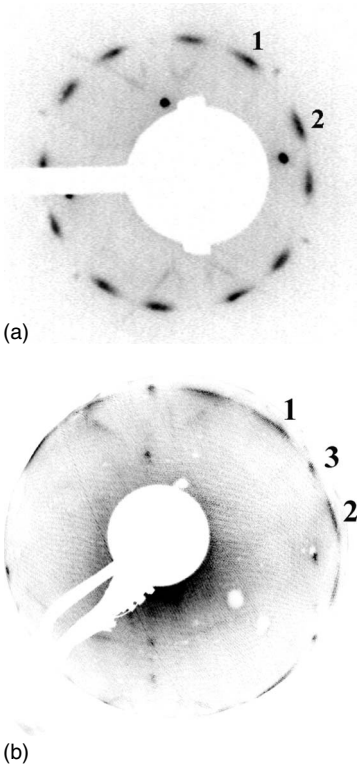

FIG. 2. LEED pattern of graphene on Ni(110). (a) Two-domain structure; (b) three-domain structure.

a series of diffraction patterns suggests that orientation 3 is absent in about one-half of the cases of graphene formation [Fig. 2(a)]. This may probably be assigned to small and difficult to control differences between the procedures used in sample preparation. The angles corresponding to the observed orientations are 0° (orientation 3) and ±13° (orientations 1 and 2) between the $[1\bar{1}0]$ direction in nickel and [1000] in graphite. It is clearly seen that the reflections from graphene are elongated in a circular fashion indicating that the domains are not well oriented with respect to the substrate. This also means that the graphene layer is incommensurate to Ni(110) substrate.

The presence in the diffraction pattern of reflection characteristic of a clean Ni surface implies that the Ni(110) face retains its structure when a graphite coating is formed. The domain structure of graphene on the Ni(110) surface is substantiated by STM observations. Figure 3(a) shows an STM image of the sample surface which illustrates the results typical of this surface. Several characteristic features stand out here. (i) The STM image reveals a pronounced Moiré pattern in the form of periodic longitudinal striations whose period may differ for different domains. This fact is in agreement with LEED observations and is explained by graphene orientational disorder. (ii) One clearly sees two regions of the surface with differently oriented Moiré patterns, which unambiguously indicates the presence of domains with different graphene orientations. (iii) A defect in the form of a step about 20 Å high is seen on the surface. As one crosses the step, the graphene orientation does not change. This implies that in passing over the defect the graphene layer, rather than becoming damaged, remains continuous. Figure 3(b) dis-

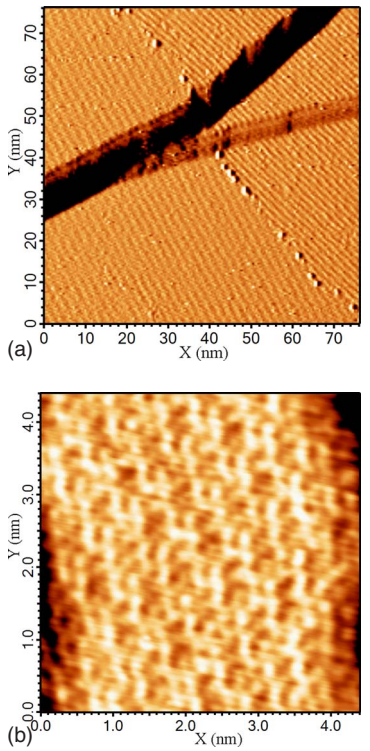

FIG. 3. (Color online) STM image of graphene on Ni(110). (a) Region of a step-shaped surface defect (current channel, $V=2$ mV, $I=27$ nA); (b) graphene viewed at high magnification (current channel, $V=3.4$ mV, $I=35$ nA).

plays an STM image of graphene on Ni(110) recorded with high resolution. Its comparison with a similar image obtained for the Ni(111) surface (Fig. 1) reveals an influence of chemical interaction between the metal surface and the carbon network on the structure of the latter. While graphene formed on Ni(111) is practically a flat film, the network on the Ni(110) surface exhibits a pronounced distortion. The film is corrugated and reproduces the profile of the metal surface. This corrugation should be distinguished from Moiré patterns mentioned above, which have periods larger than the Ni lattice constant. Based on the LEED and STM images alone, one can hardly draw well substantiated conclusions concerning the atomic structure of graphene on this surface.

B. Structure of graphene formed on faceted Ni(755) and Ni(771) surfaces

The crystal structure of graphene formed on stepped Ni(771) and Ni(755) surfaces was studied by STM and LEED. Figure 4 presents STM topographic scans of the Ni(771) and Ni(755) surfaces obtained after graphene synthesis (bright spots correspond to hillocks). In contrast to low-indexed Ni faces, the stepped surfaces exhibit a structural instability caused by interaction with carbon adsorbed on them during propylene cracking. In both cases, metal surfaces reconstruct with formation of large-area facets. An analysis shows that they are oriented along the original steps for both surfaces. The facets thus formed are nonuniform in size, with the widths reaching about 100 nm for Ni(771) and

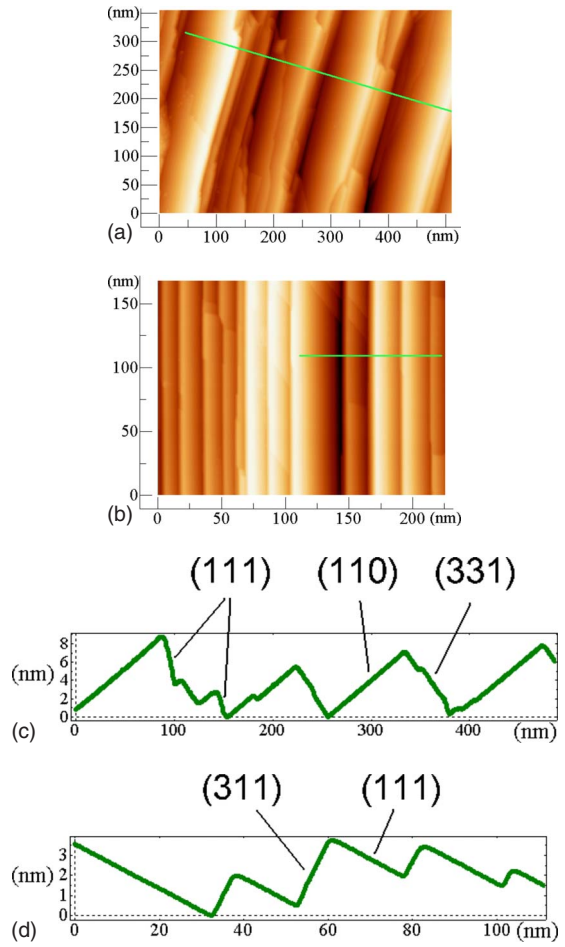

FIG. 4. (Color online) STM topographic images of (a) Ni(771) and (b) Ni(755) surface relief after formation of a graphene coating on the surface; [(c) and (d)] cross sections of the surface relief along the lines shown in panels (a) and (b).

50 nm for Ni(755). Figures 4(c) and 4(d) display a cross section of the surface relief in the directions identified with lines in Figs. 4(a) and 4(b). Most of the facets on Ni(771) are formed by the (100) basal plane and the (331) face making an angle of 13°. In addition, there are facets with an angle between the planes of 34°, which is actually the angle between the (110) and (111) faces. The cross section of the Ni(771) relief reveals facets formed by the (111) and (311) faces with an angle of 30° between them.

The LEED patterns of both surfaces exhibit two zero-order reflections denoted by (00) and produced by the two facet planes (Fig. 5). This is in complete accordance with the STM measurements and suggests that the geometry shown in Fig. 4 is characteristic of other parts of the sample surfaces as well. LEED images taken at different sample temperatures show that the topography of the surfaces obtained remains unchanged within the temperature interval of 20–480 °C.

The LEED image recorded for graphene on Ni(755) reveals hexagonally arranged nonzero-order reflections which coincide in position with those for the (111) surface and are the same for both facet sides. This suggests that (i) graphene on the (111) facet grows epitaxially, just as that on the flat Ni(111) surface and (ii) graphene on the (311) facet is ori-

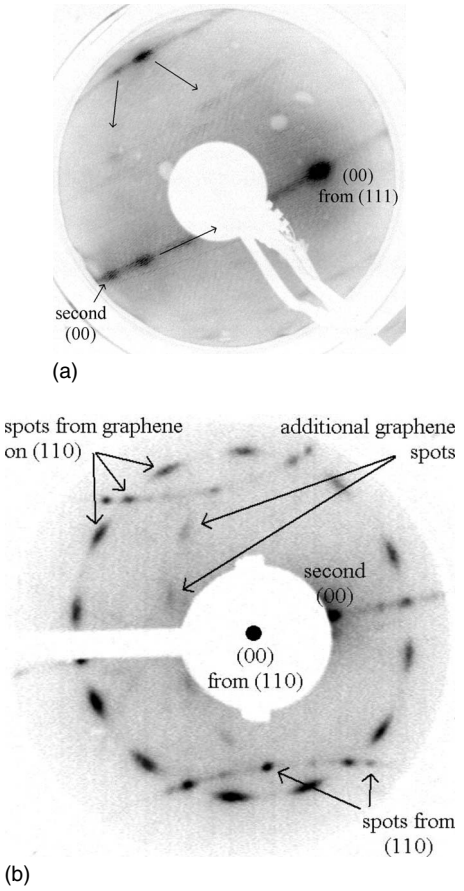

FIG. 5. LEED patterns for (a) graphene grown on Ni(755), with arrows showing the direction of reflection displacement with increasing electron kinetic energy; (b) graphene on Ni(771).

ented in the same direction as that on (111), which implies that the carbon network formed on the closely packed nickel face covers all of the sample surface with a continuous layer and interacts only weakly with the (311) face. Thus, the structure of a graphene film on the stepped Ni(755) surface is fully determined by the character of its interaction with the step terrace surface. In going from one step to another, the graphene layer skirts the facet faces while retaining its structure and orientation.

Graphene on Ni(771) exhibits a similar behavior, the only difference being that the film retains the same structure as on the (110) terrace over all of the surface. Diffraction patterns [Fig. 5(b)] exhibit weak reflections corresponding to the rectangular lattice of the Ni(110) surface. One observes also two similar series of reflections which are centered on two zero reflections and correspond to graphene layers grown on the two facet planes. A comparison with the graphene LEED pattern obtained from Ni(110) permits a conclusion that the graphene formed on the Ni(771) faceted surface has a domain structure similar to that of graphene coating a flat Ni(110) surface. The orientation of graphene on the (331) facet face coincides with that on the second (110) face, which implies that the structure of the film over all of the surface is mediated by the interaction of graphene with the substrate on the (110) terrace plane. Weak influence of both (331) and (311) facets on the graphene structure is easy to

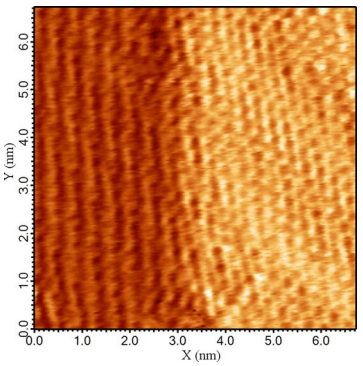

FIG. 6. (Color online) STM image of graphene formed on Ni(771) (current channel, $V=3.4$ mV, $I=28$ nA). The image is of the upper facet edge [boundary between the (110) and (331) surfaces].

understand. These surfaces consist of monoatomic steps and very short terraces. This accounts for a low interaction between the graphene and these planes.

Figure 6 presents an STM image of a part of a graphene layer on the Ni(771) surface scanned with high resolution. We readily see a boundary separating the (110) from the (331) facet planes. An analysis reveals that the graphene coating does not break at the boundary between the incommensurate parts of the surface with different crystal structures; in other words, the graphene layer coats the surface, as if it was a continuous "carpet," skirting the facet edges in the same way as the defect in Fig. 3(a). Combined with the rich variety of STM data, this permits a conclusion that domains with different graphene orientations substantially exceed in size the facet width. The continuity of the graphene coating breaks only at domain boundaries.

Recalling that the continuity of graphene coating at boundaries separating regions with structures commensurate and incommensurate to that of graphene holds for the graphene on Ni(755) as well, we arrive at the understanding that this feature is apparently common to any nickel surface and that it reflects the capacity of graphene to remain continuous on geometrically nonuniform surfaces.

A major conclusion that can be drawn from the experimental part of the present study is that it is chemical interaction of a graphene film with a metal surface that governs its structure. The interaction of graphene with the low-index (111) and (110) faces is so strong that it offsets the bending film stresses generated at terrace boundaries or at surface defects. The manifestations of this interaction, which can be traced over distances of 100–500 nm, are readily identifiable in STM images. Information on the structure of graphene on a metal at the chemical bond-length scale is rather limited. Scans recorded with high resolution cannot offer a well substantiated conclusion concerning structural details of a film. This has motivated our theoretical study undertaken to facilitate interpretation of STM data and to develop a model of the surface.

IV. THEORETICAL STUDY OF THE ATOMIC STRUCTURE OF GRAPHENE ON Ni(110)

The structure of the nickel-graphite systems was modeled using semiempirical N-body atomic interaction potentials,

which include the sum of short-range pair potentials of interatomic repulsion and of the N-body cohesion component,

$$E_{\text{tot}} = u_0 + \frac{1}{2}\sum_{A\neq B} u_{AB} - \sqrt{w_0^2 + \frac{1}{2}\sum_{A\neq B} w_{AB}^2}. \quad (1)$$

Here u_0 and w_0 are contributions which do not depend on interatomic spacings, the first of them defining the energy of noninteracting atoms and the second being proportional to the dispersion of single-electron energies of atoms making up a many-atomic system; u_{AB} and w_{AB} represent two-body atomic interactions. In their form and physical meaning, they approximate the N-body potentials obtained by combining the results obtained in the density-functional theory (DFT) formalism with those of the method of moments in tight-binding (TB) theory.[32,33] Such potentials are widely employed in studies of the properties of materials which require invoking many-atomic models of solids with a lowered symmetry of the structure, more specifically, mechanical deformation, structural stability of phases, formation and migration of defects in the bulk and on the surface of solids, etc. (see, e.g., Refs. 34–38). Two-body interactions are described in these calculations with simple functional relations whose parameters were fitted to experimental data. The potentials [Eq. (1)] were obtained in the frame of the tight-binding model with a different theoretical formalism, which makes it possible to express their components through molecular integrals and the degree of valence-shell populations.[39–41] This approach reduces the number of the fitting parameters to make them similar to those used in semiempirical methods of the quantum chemistry of the solid state. The reason for which we used this method is the structural complexity of the system, which originates from the graphite film being incommensurate to the Ni(110) surface. In the calculations, the total energy of an atomic system [Eq. (1)] was optimized in the parameters defining the crystal structure.

To test the approach, in the first stage calculations were performed for graphene on the Ni(111) surface. The major series of calculations of the equilibrium structure of a graphene film on nickel made use of the embedded-cluster model. In the case of the (111) nickel surface, the metal subsystem was modeled by a metal slab made up of five atomic layers arranged in the (111) plane. The embedded cluster of cylindrical shape included 524 atoms and the enveloping cluster 956 atoms. The substrate for the (110) surface consisted of five layers of atoms in the (110) plane. The embedded cylindrical cluster was made up of 539 atoms and the enveloping one 941 atoms. The graphite film was modeled in both cases by a disk centered on the carbon atom which included 130 atoms in the enveloping cluster.

Earlier LEED experiments,[16] as well as nonempirical calculations performed by the augmented plane-wave longitudinal-optical (APW-LO) method,[15] showed that graphene on Ni(111) is arranged preferentially in a structure in which all atoms of the first graphite sublattice are located above the metal atoms and those of the second sublattice above the hcp interstices making up straight chains. In the present study, the structure of the graphite monolayer on Ni(111) was modeled for the above preferable configuration.

TABLE I. Structure parameters of the graphite monolayer

Parameter[a]	Ni(111)			Ni(110) NP[b]
	Ref. 16	Ref. 15	NP[b]	
$d_{\max}$ (Å)	2.16 ± 0.07	2.130	2.002	1.911
$d_{\min}$ (Å)	2.11 ± 0.07	2.122	1.659	1.342

[a] $d_{\max}, d_{\min}$—maximum and minimum distances to the substrate.
[b] NP—N-body potential calculation.

The geometry of an adsorbed film was optimized in three parameters, namely, in the compression coefficient and distances of carbon atoms on the first and second sublattices to the face. Table I lists the results of our calculations together with the data reported in Refs. 15 and 16.

The distances of the graphene sublattices to the metal surface obtained in our calculations are somewhat smaller than the experimental values. Film deformation involving transfer of each second carbon atom to the trigonal interstitial position is more pronounced. Nevertheless, the main features of the monolayer structure are reproduced qualitatively correctly.

A feature that makes the graphene/Ni(110) system essentially different from the graphene/Ni(111) lies in the hexagonal carbon network being incommensurate to the rectangular corrugated metal lattice the structure of which is presented in Fig. 7. This does not permit one to advance any preliminary assumptions concerning the orientation of a graphite monolayer on a metal surface based on system symmetry alone. At the same time, LEED and STM data reveal a fairly regular and reproducible structure of the graphite monolayer on the Ni(110) surface.

The structure of a graphite monolayer on Ni(110) was modeled by the following scheme. The center of a 130-atom fragment of graphite was placed at different points in the irreducible region of the two-dimensional (110) metal cell, which is shaped as a right-angled triangle (Fig. 7). The dependence of the total energy of the system on the rotation angle of the film was calculated for each point with a step of 0.66°. The total energy was optimized in two parameters. The first parameter was the distance from the film to the metal surface. Because interaction of carbon with the substrate may bring about deformation of the graphene layer, we used for the second parameter the amplitude of sinusoidal

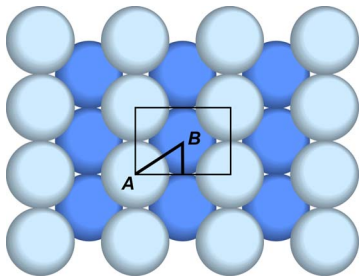

FIG. 7. (Color online) Structure of the Ni(110) surface. Thick solid lines identify the irreducible region of the two-dimensional lattice cell. Points A and B on the cell diagonal correspond to $\lambda = 0$ and $\lambda = 1$, respectively.

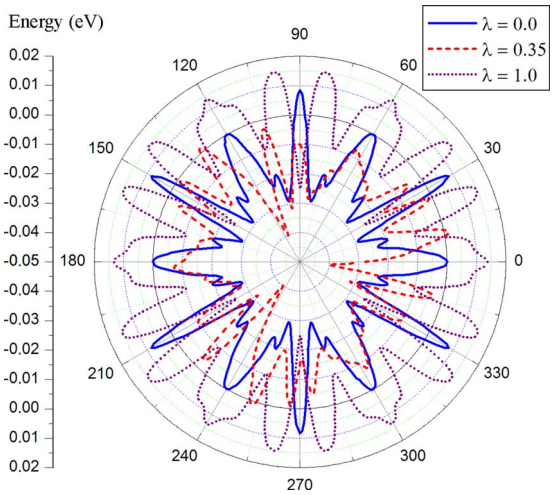

FIG. 8. (Color online) Total energy of graphene/Ni system normalized to the number of carbon atoms and plotted vs graphene film rotation angle for different positions of the center of rotation on the diagonal of a two-dimensional cell ($\lambda=0,0.35,1.0$). Zero energy corresponds to zero rotation angle (one of the C-C bonds of central carbon atom is oriented along the $[1\bar{1}0]$ direction) and $\lambda=0$ (central carbon atom is located above Ni atom). Embedded graphene cluster used in calculations included 67 carbon atoms.

deformation of the carbon network, the period of which was that of the corrugations on the nickel surface. The interatomic distances in graphene were assumed to be the same as those on the Ni(111) surface.

The angular dependences of total energy have a complex shape. In Fig. 8, they are shown graphically for three points lying on the diagonal of the two-dimensional lattice cell of the metal (the point positions are specified by the parameter λ). For other points these dependences exhibit a similar character. The number of their minima corresponds to the number of the closest-packed graphene rays which are directed along the carbon-carbon bonds, as well as along the zigzag carbon atom chains, i.e., at an angle of 30° to the bond directions. There are 12 such rays altogether, and the extrema of the potential curves correspond to a particular orientation of these rays with respect to the surface corrugations.

An analysis of the relative depths of the absolute minima in the angular energy dependences constructed for different points of the cell suggests the existence of two minima on the potential surface. The first of them refers to the position of the film in which its central atom is located just above the nickel atom, and the film is turned such that one of the bonds of the central carbon atom makes an angle of 16° with the $[1\bar{1}0]$ direction. The total energy of the system increases with the film displaced from this position in any direction. As follows from calculations (Fig. 9), deformation of a film induced by its interaction with nickel complicates markedly the atomic structure of graphene. The structural parameters for this optimal structure ($\lambda=0$) are listed in Table I. The maximum metal-graphite distance in this structure is smaller by 5% than the distance found for the Ni(111) surface. The film orientation on the metal surface for this structure is close to that derived from LEED measurements. The graphite film is the closest to the metal surface near the corrugation bottom, where it is drawn in by 0.57 Å.

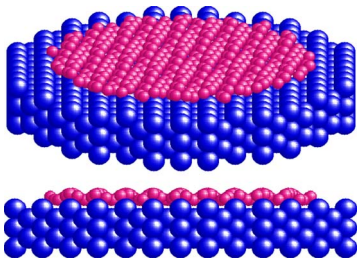

FIG. 9. (Color online) Atomic structure of a graphite layer on the nickel (110) surface as derived from calculations.

The second minimum of the potential surface was found to exist for an asymmetrically located center of the 130-atom graphite fragment, which lies on the diagonal of the metal lattice cell, at a distance of 0.35 of its length from the corner to the center of the rectangle. The angle made in this structure by the C-C bond of the central carbon atom with the $[1\bar{1}0]$ direction is substantially smaller (not over 6°). This means that the zigzag carbon chains lie in the corrugations formed by atomic rows on the metal surface in the [001] direction. This structure turns out to be energetically somewhat preferable to the first one.

To reveal the extent to which the results obtained depend on the choice of the graphene film model, additional calculations were performed for both low-energy structures with different numbers of carbon atoms (13, 37, and 103 atoms) in the embedded cluster (with the size of the 130-atom enveloping cluster kept unchanged). In all the cases, the extrema of the potential curves turn out to be located at about the same film rotation angles although the relative positions of extrema on the energy scale vary among the clusters considered. This confirms the suggestion that the stability of film orientation depends on mutual positions of closely packed carbon atom rays and corrugations on the metal surface.

Turning now back to a discussion of the two possible orientations of a graphite monolayer, a few points may appear to be in order. Although calculations suggest that the second of the two optimal structures has a lower energy, formation of the first structure, which is actually observed in most experiments, can result from the kinetics of graphene growth. At the initial instant of monolayer formation, the first carbon atom to be adsorbed becomes fixed above a metal atom, which can be attributed to creation of a covalent σ bond through overlap of the nickel d orbital with the π orbital of carbon. The film expands in growing around this "reference" atom. After this nucleus of the film has formed, its displacement to an energetically more favorable position may turn out hampered by the energy barrier separating the two local energy minima (Fig. 10). Therefore, the graphite monolayer will, as a rule, continue to grow in its first orientation.

V. CONCLUSION

Commensurate and incommensurate graphene coatings on flat nickel (111) and (110) surfaces, accordingly, as well as

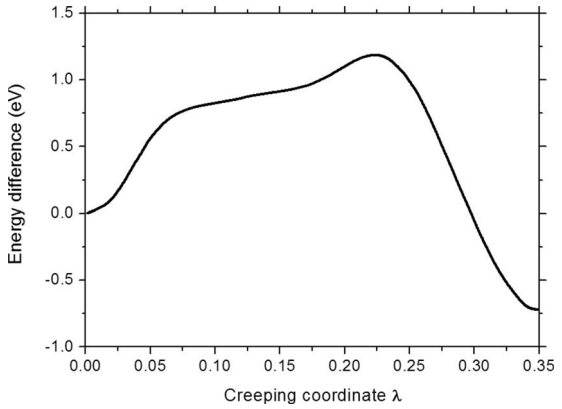

FIG. 10. Binding energy of a C67 embedded graphene cluster plotted vs generalized "creeping" coordinate (displacement along the diagonal of a two-dimensional cell combined with rotation).

on stepped Ni(771) and Ni(755) surfaces, have been studied by STM and LEED. Studies of graphene synthesized on flat surfaces have revealed that, in contrast to graphene on Ni(111), which forms a continuous single-crystal (1×1) coating, the graphene grown on the Ni(110) surface has a complex incommensurate crystal structure modified markedly by interaction with the substrate. A theoretical analysis has been undertaken to describe the graphene structure on this surface. As shown by the calculations, the fairly strong chemical interaction of carbon with nickel curves notice a graphene layer on a scale of a few angstroms. Its crystal structure becomes modulated with the substrate lattice period of 3.5 Å with an amplitude of 0.57 Å, quite a noticeable value compared with the interatomic spacing in graphene. The lattice constant of graphene differs very little from that of bulk graphite. Stable orientations of the graphite monolayer on Ni(110) correspond to certain fixed angles between the $[1\bar{1}0]$ direction of atomic rows on the metal surface and 12 closest-packed graphene rays, which are directed along the C-C bonds as well as along the zigzag chains of carbon atoms. This model of the atomic structure of graphite permitted proper interpretation of the STM data. Strong deformation of the graphene crystal structure caused by interaction with Ni substrate should have a significant influence on the graphene valence-band electronic structure. The changes in energy dispersions should appear not only in the form of π bands shift toward higher binding energies reported elsewhere[17,31] for different Ni surfaces; we suppose that there should be effects caused by graphene structure modulation with the period of substrate.

Studies of graphene grown on stepped Ni(771) and Ni(755) surfaces reveal that formation of such a coating by the propylene cracking technique involves faceting of both substrates along a closest-packed nickel single-crystal faces which approach closest in the angle to the basal surface of the original step terraces. It has been found that the orientation of graphene with respect to the substrate is fully determined by its orientation on the basal close-packed surface. The orientation of graphene on Ni(755) coincides with that on Ni(111). Graphene grown on Ni(771), similar to the Ni(110) case, has a domain structure with three most preferred directions of orientation. The size of the domains exceeds by far the characteristic size of the facets. The data obtained have led us to the conclusion that despite the complex and geometrically nonuniform relief of faceted surfaces, a graphene layer does not break at facet edges where different crystallographic planes of the substrate meet. The same property was found for a thin graphite film formed on a SiC substrate in Ref. 42. This is made possible by the curving of graphene, a process requiring an energy that, as shown by the calculations, is counterbalanced by the strong interaction with the substrate.

ACKNOWLEDGMENTS

This work was supported by RFFI (Projects No. 08-03-00410 and No. 07-02-00809) and FCP (Contracts No. 02.518.11.7029, No. 02.513.11.3355, and No. SS-5902.2008.2).

*usachov.d@mail.ru

[1] N. B. Hannay, T. H. Geballe, B. T. Matthias, K. Andres, P. Schmidt, and D. MacNair, Phys. Rev. Lett. **14**, 225 (1965).
[2] Z. K. Tang, Lingyun Zhang, N. Wang, X. X. Zhang, G. H. Wen, G. D. Li, J. N. Wang, C. T. Chan, and Ping Sheng, Science **292**, 2462 (2001).
[3] T. E. Weller, M. Ellerby, S. S. Saxena, R. P. Smith, and N. T. Skipper, Nat. Phys. **1**, 39 (2005).
[4] K. S. Novoselov, A. K. Geim, S. V. Morozov, D. Jiang, M. I. Katsnelson, I. V. Grigorieva, S. V. Dubonos, and A. A. Firsov, Nature (London) **438**, 197 (2005).
[5] Y. Zhang, Y.-W. Tan, H. L. Stormer, and P. Kim, Nature (London) **438**, 201 (2005).
[6] K. S. Novoselov, Z. Jiang, Y. Zhang, S. V. Morozov, H. L. Stormer, U. Zeitler, J. C. Maan, G. S. Boebinger, P. Kim, and A. K. Geim, Science **315**, 1379 (2007).
[7] K. S. Novoselov, E. McCann, S. V. Morozov, V. I. Fal'ko, M. I. Katsnelson, U. Zeitler, D. Jiang, F. Schedin, and A. K. Geim, Nat. Phys. **2**, 177 (2006).
[8] K. S. Novoselov, A. K. Geim, S. V. Morozov, D. Jiang, Y. Zhang, S. V. Dubonos, I. V. Grigorieva, and A. A. Firsov, Science **306**, 666 (2004).
[9] C. Berger, Zhimin Song, Tianbo Li, Xuebin Li, A. Y. Ogbazghi, Rui Feng, Zhenting Dai, A. N. Marchenkov, E. H. Conrad, P. N. First, and W. A. de Heer, J. Phys. Chem. B **108**, 19912 (2004).
[10] T. Ohta, A. Bostwick, T. Seyller, K. Horn, and E. Rotenberg, Science **313**, 951 (2006).
[11] O. V. Krylov, *Heterogeneous Catalysis* (Akademkniga, Moscow, 2004) (in Russian).
[12] J. Sehested, Catal. Today **111**, 103 (2006).
[13] H. S. Bengaard, J. K. Norskov, J. Sehested, B. S. Clausen, L. P. Nielsen, A. M. Molenbroek, and J. R. Rostrup-Nielsen, J. Catal.

209, 365 (2002).
[14] R. Koch, O. Haase, M. Borbonus, and K.-H. Rieder, Phys. Rev. B **45**, 1525 (1992).
[15] G. Bertoni, L. Calmels, A. Altibelli, and V. Serin, Phys. Rev. B **71**, 075402 (2005).
[16] Y. Gamo, A. Nagashima, M. Wakabayashi, M. Terai, and C. Oshima, Surf. Sci. **374**, 61 (1997).
[17] A. Nagashima, N. Tejima, and C. Oshima, Phys. Rev. B **50**, 17487 (1994).
[18] K. Yamamoto, M. Fukushima, T. Osaka, and C. Oshima, Phys. Rev. B **45**, 11358 (1992).
[19] A. M. Shikin, D. Farías, and K.-H. Rieder, Europhys. Lett. **44**, 44 (1998).
[20] A. M. Shikin, D. Farías, V. K. Adamchuk, and K.-H. Rieder, Surf. Sci. **424**, 155 (1999).
[21] Yu. S. Dedkov, A. M. Shikin, V. K. Adamchuk, S. L. Molodtsov, C. Laubschat, A. Bauer, and G. Kaindl, Phys. Rev. B **64**, 035405 (2001).
[22] D. Farías, A. M. Shikin, K.-H. Rieder, and Yu. S. Dedkov, J. Phys.: Condens. Matter **11**, 8453 (1999).
[23] D. Farías, K.-H. Rieder, A. M. Shikin, V. K. Adamchuk, T. Tanaka, and C. Oshima, Surf. Sci. **454**, 437 (2000).
[24] A. M. Shikin, M. V. Poigin, Y. S. Dedkov, S. L. Molodtsov, and V. K. Adamchuk, Fiz. Tverd. Tela (Leningrad) **42**, 1134 (2000) [Phys. Solid State **42**, 1170 (2000)].
[25] A. G. Starodubov, M. A. Medvetskii, A. M. Shikin, and V. K. Adamchuk, Fiz. Tverd. Tela (Leningrad) **46**, 1300 (2004)[Phys. Solid State **46**, 1340 (2004)].
[26] A. M. Shikin, S. A. Gorovikov, V. K. Adamchuk, W. Gudat, and O. Rader, Phys. Rev. Lett. **90**, 256803 (2003).
[27] A. M. Shikin, G. V. Prudnikova, V. K. Adamchuk, W.-H. Soe, K.-H. Rieder, S. L. Molodtsov, and C. Laubschat, Fiz. Tverd. Tela (Leningrad) **44**, 652 (2002) [Phys. Solid State **44**, 677 (2002)].
[28] W. H. Soe, A. M. Shikin, F. Moresco, V. K. Adamchuk, and K. H. Rieder, Phys. Rev. B **64**, 235404 (2001).
[29] A. M. Shikin, G. V. Prudnikova, V. K. Adamchuk, F. Moresco, and K.-H. Rieder, Phys. Rev. B **62**, 13202 (2000).
[30] V. Saltas and C. A. Papageorgopoulos, Surf. Sci. **488**, 23 (2001).
[31] D. Yu. Usachov, A. M. Shikin, A. Yu. Varykhalov, V. K. Adamchuk, and O. Rader, Fiz. Tverd. Tela (Leningrad) **49**, 899 (2007) [Phys. Solid State **49**, 949 (2007)].
[32] M. W. Finnis and J. E. Sinclair, Philos. Mag. A **50**, 45 (1984).
[33] A. P. Sutton and J. Chen, Philos. Mag. Lett. **61**, 139 (1990).
[34] R. M. Lynden-Bell, J. Phys.: Condens. Matter **7**, 4603 (1995).
[35] L. Gomez, A. Dobry, and H. T. Diep, Phys. Rev. B **55**, 6265 (1997).
[36] M. I. Baskes, Phys. Rev. Lett. **83**, 2592 (1999).
[37] Y. Mishin, D. Farkas, M. J. Mehl, and D. A. Papaconstantopoulos, Phys. Rev. B **59**, 3393 (1999).
[38] T. Çağin, G. Dereli, M. Uludogan, and M. Tomak, Phys. Rev. B **59**, 3468 (1999).
[39] A. M. Dobrotvorskii, Teor. Eksp. Khim. **27**, 437 (1991) (in Russian).
[40] A. M. Dobrotvorskii and O. V. Afanasjeva, J. Phys.: Condens. Matter **5**, 8839 (1993).
[41] A. M. Dobrotvorskii and V. K. Adamchuk, Zh. Tekh. Fiz. **64**, 132 (1994) (In Russian).
[42] Th. Seyller, K. V. Emtsev, K. Gao, F. Speck, L. Ley, A. Tadich, L. Broekman, J. D. Riley, R. C. G. Leckey, O. Rader, A. Varykhalov, and A. M. Shikin, Surf. Sci. **600**, 3906 (2006).